Predicting Total Harmonic Distortion in Asymmetric Digital Subscriber Line Transformers by Simulation

Peter R. Wilson, *Member, IEEE*, J. Neil Ross, and Andrew D. Brown, *Senior Member, IEEE*

***Abstract*—As a design application, the asymmetric digital subscriber line (ADSL) broad-band line transformer offers somewhat different challenges than those in power supply design. In this paper, we use simulation to analyze total harmonic distortion (THD) as affected by the nonlinear behavior of the magnetic material in a line transformer. We use a mixed-technology model of the line transformer and circuit simulation to predict the level of THD for a variety of core types and configurations. A comparison of the simulation results with measured THD figures demonstrates the accuracy of the models.**

***Index Terms*—Asymmetric digital subscriber line (ADSL), hysteresis, modeling, simulation, total harmonic distortion (THD).**

I. Introduction

DESPITE the ever increasing integration of broad-band modem integrated circuits for technologies such as asymmetric digital subscriber line (ADSL), there is still a need for a line transformer to isolate the line from the device at either the central office (CO) or customer premises.

A crucial design problem for the manufacturers of such components is the total harmonic distortion (THD) that will result when the component is placed in the complete system, and how much is due to the nonlinearities introduced by the magnetic component itself. As a result, it has become highly desirable to apply modeling techniques commonly used in power applications, such as switch mode power supplies, i.e., the use of nonlinear magnetic material models, to assess the potential THD for a particular design.

In this paper, a commonly used nonlinear magnetic material model, the Jiles–Atherton model, is used to estimate the THD performance of a variety of line transformers.

II. Background

A. Introduction to ADSL

ADSL technology is used as a high-speed modem link with asymmetric up- and down-stream data rates as the name suggests. The current primary application is for very high-speed Internet access, but the goal of the technology is not restricted to purely Internet applications, but also video-streaming (for commercial video-on-demand), fast data transfer, and fully integrated network services for companies and home use.

Manuscript received August 13, 2002; revised February 19, 2004. This work was supported in part by Advanced Power Components, Rochester, U.K.

The authors are with the Department of Electronics and Computer Science, University of Southampton, Southampton SO17 1BJ, U.K. (e-mail: prw@ecs.soton.ac.uk; jnr@ecs.soton.ac.uk; adb@ecs.soton.ac.uk).

Digital Object Identifier 10.1109/TMAG.2004.826907

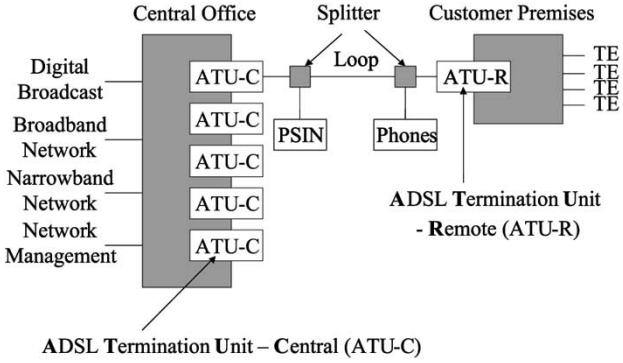

Fig. 1. ADSL network configuration outline.

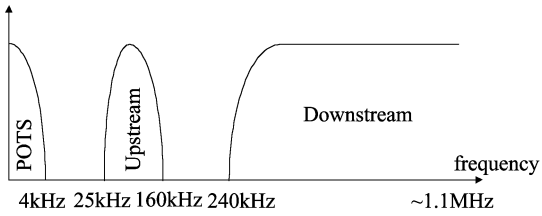

Fig. 2. ADSL bandwidth allocation.

A significant differentiator between ADSL and current cable television access is the ability to utilize the existing infrastructure (i.e., copper twisted-pair wires) of the telephone network. Fig. 1 shows the outline of a typical network configuration, with a CO connection at the service provider, and a number of remote customer premises equipment (CPE) installations.

ADSL has proved a significant step in the development of digital subscriber line (DSL) technology, as it has probably the best defined standard (IEEE Standard T1.413-1995 [1]) that is actually implemented de facto in the telecommunications industry, by both service providers and chip manufacturers alike. Bingham [2] and Cioffi [3] describe the development of the philosophy for ADSL and similar broad-band approaches, and Goralski [4] and Chen [5] provide background to the technology area to high-speed communications. It is beyond the scope of this paper to go into detail of the mechanism of the ADSL system, but it is useful to describe some details of the transmission scheme and the analog interface to understand the requirements for ADSL line transformers.

B. ADSL Modulation Scheme

ADSL is based on a broad-band modulation scheme, with multiple carriers placed at 4.3125-kHz intervals. With 256 carriers, a 1.1-MHz bandwidth is required. These subcarriers may also be referred to as subchannels. Fig. 2 shows how the bandwidth is divided into areas for the standard telephone commu-

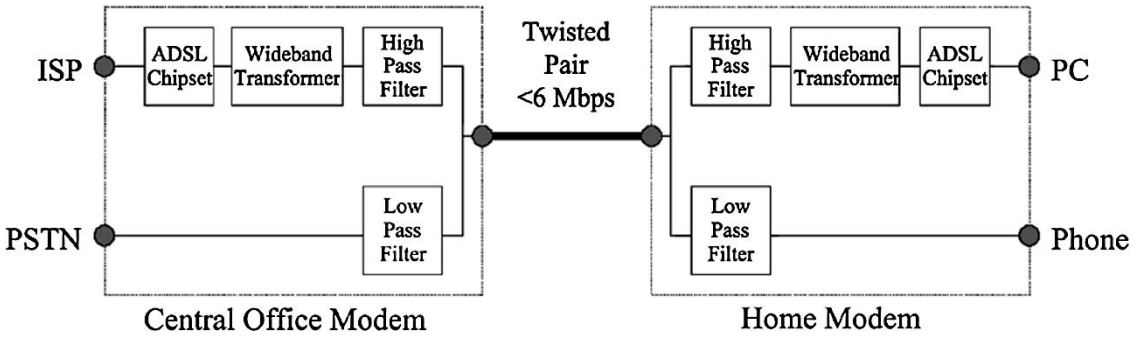

Fig. 3. ADSL analog interface.

nications (POTS), up-stream and down-stream bandwidth. In Fig. 2, with the distinct gap in the bandwidth between the up- and down-streams, there is no requirement for echo cancellation. If echo cancellation is used, then a more efficient use of the bandwidth occurs where the up- and down-streams overlap.

Two methods of modulation can be used in ADSL: carrierless amplitude/phase modulation (CAP), and discrete multitone modulation (DMT). CAP is very similar to quadrature amplitude modulation (QAM), except that the carrier itself is not transmitted. The carrier does not actually hold any information and is therefore recreated at the receiver for efficiency. The phase is synchronized using phase sequences in the data.

DMT is the method described in the ANSI Standard T1.413, and uses intelligent allocation of the different channels to send the appropriate number of bits to achieve maximum overall throughput. Each individual channel uses QAM, so although both CAP and DMT use QAM at the lowest level, the difference is the dynamic allocation of data to individual channels using DMT that provides a potentially better data rate.

C. Overview of the Analog Interface and Modeling Line Transformers

As has been described in the previous section, the signals to be transmitted between two ADSL modems are modulated using some form of QAM, with an interface between the modem hybrid and the line of a 1 : 1 line transformer, as shown in Fig. 3.

Day *et al.* [6] provide an excellent primer in the design of ADSL hybrids, and address some of the rudimentary aspects of the transformer design. Other useful and practical sources of design information can be found in work by Cornil [7] and Cabler [8]. The key issues are loss, matching, parasitic effects, and distortion. The frequency response is limited at low frequencies by the magnetizing inductance. The parasitic leakage inductance and winding capacitance reduce the bandwidth at higher frequencies. Resistive losses in the windings also provide a source of loss in the device across the whole range. The overall effect on the insertion loss is summarized in Fig. 4.

Steffes [9] and Nash [10] demonstrate how simulating the line driver and its associated circuitry can predict the performance of the analog interface in general. Day and Wurcer [6] and Dean [11] have shown specifically how a simple model of a transformer, including the parasitics as shown in Fig. 5, can be used to predict the frequency response and insertion loss of the device. This is shown in Fig. 6, with a graph of the simulated insertion loss for a realistic ADSL device.

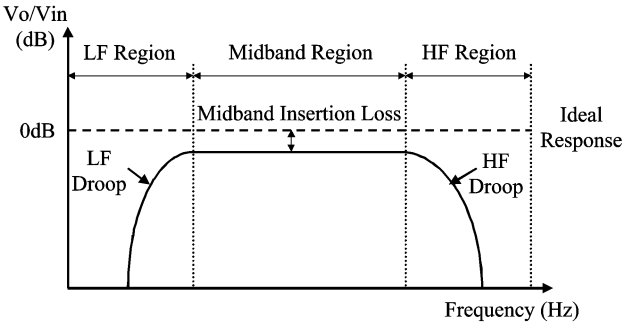

Fig. 4. Transformer insertion loss with nonideal model.

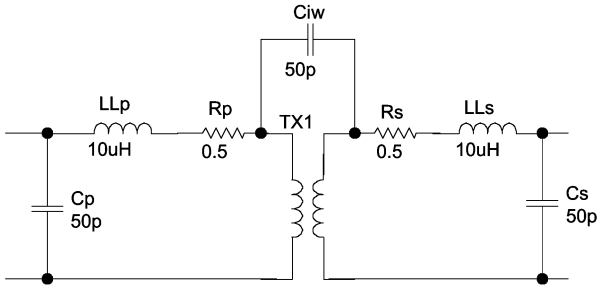

Fig. 5. Transformer model used for simulation of insertion loss.

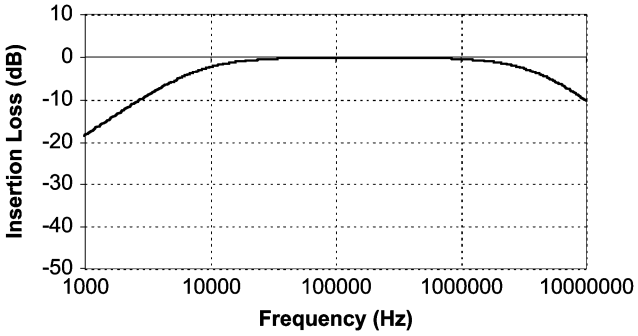

Fig. 6. Simulated insertion loss.

Using simulation in this way is an effective tool in identifying critical parameters, defining parametric limits, and optimizing device performance.

In order to achieve effective and accurate simulation results, it is necessary to characterize these parameters accurately as has been discussed previously in this paper. The range of methods employed range from analytical approaches, such as those proposed by Dowell [12], Dauhajre [13], [14], and Snelling [15], through to integrated modeling procedures involving multiple finite-element analyses (FEA), such as those

described by Asensi *et al.* [16]–[18], Wilson [19], Lopera *et al.* [20] and Prieto *et al.* [21]–[24].

The other issue with the transformer is its effect on signal distortion. If distortion occurs in a subcarrier or channel, then degradation of the signal may occur, giving rise to loss of signal integrity and data errors. A further side effect of nonlinearities in the core is the possible introduction of intermodulation products in other subcarriers or channels. Even if the transformer is designed to operate largely in a linear region, due to the nature of the modulation scheme used in ADSL, large peak-to-average ratios (PAR) may occur giving rise to significant magnetic offsets and possible nonlinear behavior. Tellado [25] discusses the potential for large PAR in ADSL systems in some detail, and also methods for its reduction. Due to the broad-band nature of the signals, phase shifts may also occur in the transmitted signal, as a result of different frequencies across the range having a different phase response in the core material. This may also result in phase shifts in the recovered ADSL signals.

It is important, therefore, in a simulation model to include the nonlinear core model to ensure that the transformer does not degrade the performance of the system as a whole. This paper concentrates on this aspect of the transformer design, with investigations carried out into the tradeoffs of material characteristics and air gaps, the effect of core size and number of windings on performance, and comparisons between different winding configurations and core types. Previous work [26] describes the basic design procedure for DSL transformers, but relies on "rule of thumb" calculations and simplification of the THD figures. It is proposed in this paper to apply circuit simulation to more accurately predict the effect of nonlinear ferrite cores on the transformer's performance. The proposed model will have a similar parasitic model to that described previously, but will include an accurately characterized nonlinear core model. In this case, the original Jiles–Atherton [27]–[29] model has generally been used. The modifications to the Jiles–Atherton model that have been proposed previously by Wilson *et al.* [30]–[33] generally refer to heavily saturated cores, and in general the ADSL transformers operate at low signal levels implying minor B–H loops.

D. Distortion Performance Criteria

There are several criteria that are used to measure the performance of DSL transformers, including THD and signal-to-noise ratio (SNR). This section defines these criteria as they have been used in this work. The THD figure is of primary interest to ADSL system designers and is usually the only distortion figure given on a data sheet.

THD is used to establish the effect on an ideal sinusoidal test tone of nonlinearities in the transformer. The THD is calculated using

$$\text{THD} = \frac{\sqrt{\sum_{i=2}^{5} V_i}}{V_1} \tag{1}$$

where V_1 is the peak harmonic, the voltage at the ideal tone frequency, and V_2, V_3, V_4, V_5 are the second through fifth harmonics, respectively. A variation on the THD is the THD+Noise figure, which extends the range of harmonics to include all the harmonics measured. This is similar to the SNR and is calculated using

$$\text{SNR} = \frac{V_1(\text{rms})}{\sum_{i=2}^{n} V_i(\text{rms})} \tag{2}$$

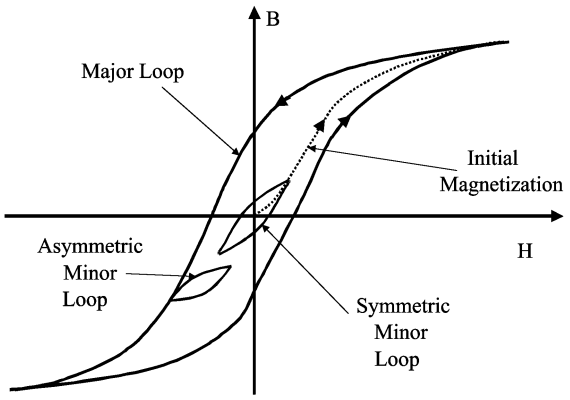

Fig. 7. Nonlinear B–H behavior in transformer core.

III. Distortion in Transformers Due to Nonlinear Magnetic Materials

A. Introduction

Having defined the measurement criteria for distortion, it is useful at this stage to consider the sources of distortion, and how simulating transformers could predict the level of distortion. Due to the nonlinear nature of the transformer ferrite core, the voltage waveforms on the windings will have a nonlinear relationship with respect to the current through the driving (primary) windings. This is due to the nonlinear relationship between B and H in the core. Fig. 7 illustrates how the B–H characteristic changes as the applied field strength (H) is increased, introducing nonlinear behavior.

Near the origin, the relationship between B and H is essentially linear, but as H increases, the slope of the B–H curve steepens until saturation occurs, at which point the slope reduces once again (this is clearly seen on the initial magnetization curve). This illustrates how there are two potential sources of distortion, at low and high field strengths. Fig. 7 also shows how any magnetic offset conditions may cause different slopes and sizes of loop, as shown with the minor loop variations.

B. Modeling Hysteresis Using a Mixed-Technology Approach

This behavior can be modeled in transformers using a mixed-domain approach with the hysteresis modeled in the magnetic domain connected to the electrical domain using winding models. The resulting voltage waveforms reflect the effect of the nonlinear behavior of the core. This approach is well understood and has been described by Cherry [34], Laithwaite [35], and Carpenter [36]. More specifically, the use of detailed hysteresis models in the magnetic domain in conjunction with electrical circuit models are described by Brown *et al.* [37] and Wilson [38]. As long as accurate models of the core nonlinearity are used, then it is possible to estimate the effect on distortion of the voltage waveforms. A common

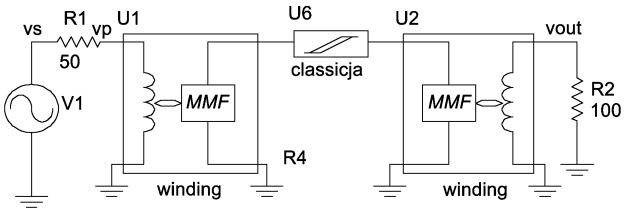

Fig. 8. Transformer mixed-technology model and test circuit.

assumption in the available design guides from manufacturers such as Ferroxcube [26] indicates that the third harmonic is the only significant problem in DSL transformer design, but this assumes that hysteresis is not taking place in the core. If hysteresis is included, then the second through to the fifth harmonic may have an impact on the transformer performance. In the testing and simulation that follows, all the harmonics are considered, not just the third.

The general approach to modeling a transformer using mixed technology model is shown in Fig. 8, with a two winding transformer modeled using two winding models and a single nonlinear core model in the magnetic domain.

The crucial part of the model for accurate prediction of the nonlinear behavior at the device terminals is the nonlinear core model in the magnetic domain. As has been discussed previously, the focus in ADSL applications is on low signal levels, with minimal distortion, and so accurate minor loop modeling is important. Carpenter [39] and Jiles [40] have described how a model can be produced, based on the original Jiles–Atherton model, that can accurately replicate the minor loop behavior, while Wilson and Ross [31] demonstrate how appropriate characterization and optimization of the model can provide a best fit of the model's behavior under these specific conditions.

C. Source of Distortion in the Electrical Domain

The source of the distortion apparent in the electrical domain is the nonlinearities in the magnetic domain. This may be a problem in understanding the direct effect of a particular aspect of the magnetic material behavior on the resulting electrical waveforms. This is due in part to the fact that the voltage across a winding is in fact the derivative of the flux (and flux density) in the magnetic material. In order to aid the understanding of the waveform shapes, a typical model is used and the applied field strength gradually increased so that the B–H loop becomes progressively more saturated. The resulting waveforms can be analyzed to observe the effect on the voltage across the terminals of the magnetic component in the electrical domain. By applying a fixed field strength with values of 1, 10, and 50 A/m for a core model characterized with the material 3E6, the B–H curves, resulting voltage waveforms for an ideal winding with a single turn, and the Fourier coefficients can be calculated. The resulting B–H curves are shown in Figs. 9–11.

It is clear from these figures that as the field strength increases from 1 to 50 A/m, the B–H curve first develops a small hysteresis loop and as the material nears saturation, there is the transition into a major loop shape with distortion at the loop tips. The effect this has on the resulting voltage on the winding terminals is shown in Figs. 12–14.

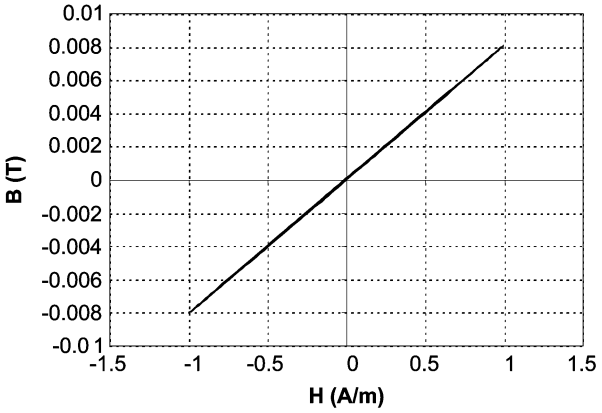

Fig. 9. Simulated B–H curve for 3E6 material with $H_{\max} = 1$ A/m.

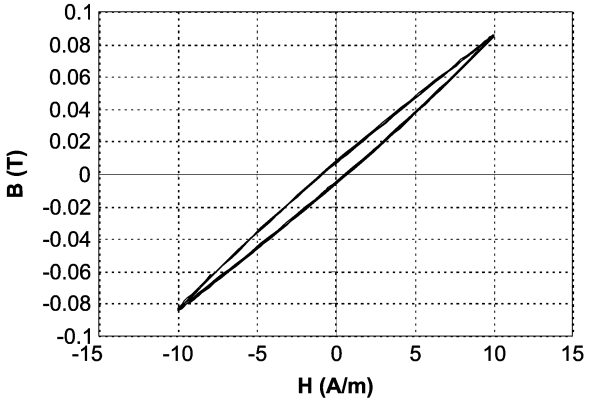

Fig. 10. Simulated B–H curve for 3E6 material with $H_{\max} = 10$ A/m.

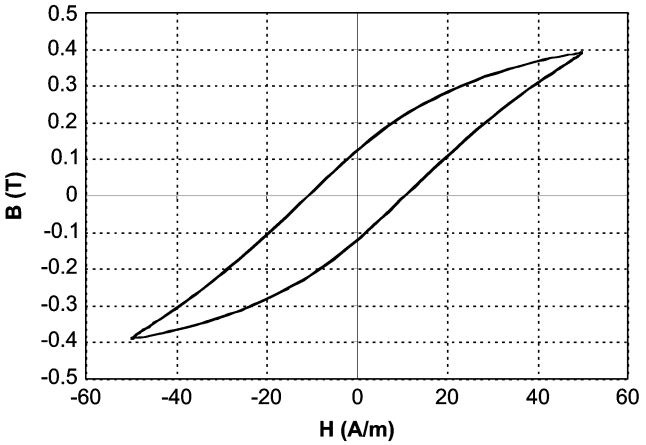

Fig. 11. Simulated B–H curve for 3E6 material with $H_{\max} = 50$ A/m.

It is clear that by the time the applied field strength has reached 50 A/m, there is significant distortion of the voltage waveform on the winding. In order to quantify the levels of distortion, and to compare between different levels of applied signal, the normalized harmonics were calculated using a discrete Fourier transform (DFT) and are shown in Fig. 15.

Fig. 15 clearly shows the increase in harmonic level as the core material goes more into saturation at higher applied field strengths. This is quantified in Table I, which shows the relationship between the applied field strength and the calculated THD level on the output voltage waveforms.

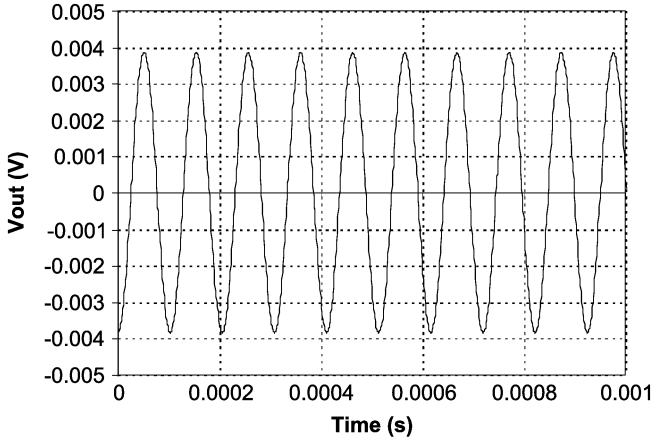

Fig. 12. Simulated voltage for 3E6 material with $H_{\max} = 1$ A/m.

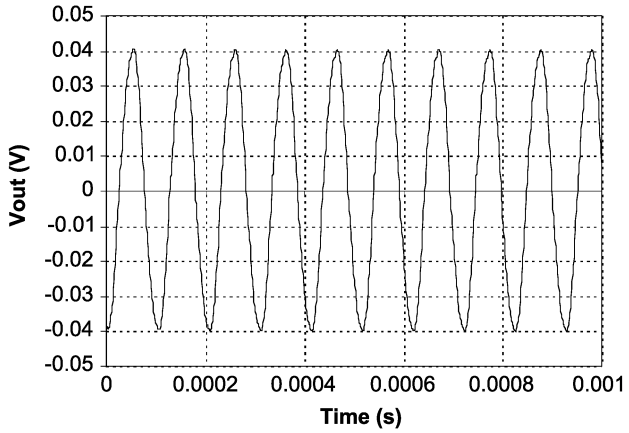

Fig. 13. Simulated voltage for 3E6 material with $H_{\max} = 10$ A/m.

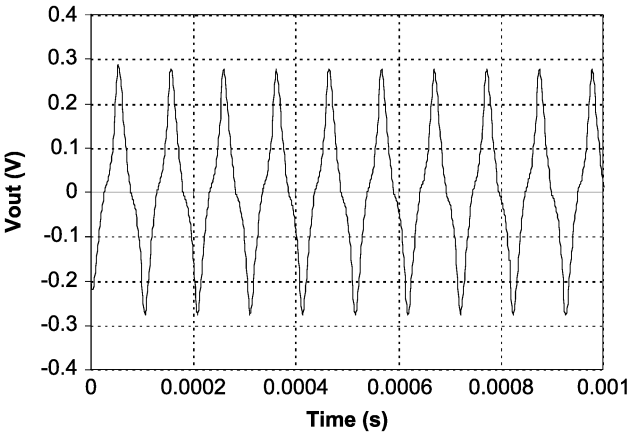

Fig. 14. Simulated voltage for 3E6 material with $H_{\max} = 50$ A/m.

Using this general approach, specific cases of transformer can be tested and the THD compared with measured values.

IV. Predicting Total Harmonic Distortion (THD) With Simulation

A. Introduction

In order to investigate the techniques required to simulate the THD performance of a line transformer for ADSL, a series of transformers was constructed, THD measured, and models were derived and simulated. Comparisons were made between the measured and simulated results to assess the accuracy of the simulation model and its usefulness for predicting the THD figure for a variety of transformer configurations. Gapped and ungapped cores were chosen to establish the effect of air gaps on the performance, and similarly toroidal (ring) cores were compared with two-piece (ER11) cores. The types of core used in this section were a TN10/6/4 toroid and ER11 (gapped and ungapped). All of the cores were made of the materials 3E5 or 3E6 (Philips), or T38 (Siemens).

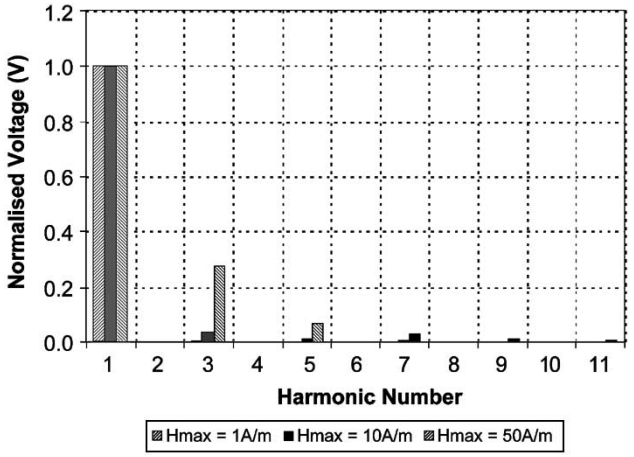

Fig. 15. Normalized harmonics for $H_{\max} = 1$, 10, and 50 A/m.

TABLE I
Relationship Between Applied Field Strength and THD

Hmax (A/m)	THD (%)
1	0.38
10	4.05
50	28.4

TABLE II
3E5 Model Parameters

Parameter	Value
a	5.245
k	20.022
c	1.1675
α	4.1u
M_s	241k

B. Toroid TN10/6/4-3E5 Line Transformer

The first test case was a TN10/6/4 toroid made of 3E5 material. The component was a two-winding transformer, each winding wound with 60 turns of 28 s.w.g wire. To ensure accurate results, a 12-bit oscilloscope was used to enable more accurate definition of small signal harmonics (the Tektronix TDS220 oscilloscope used previously in this work has only 8-bit resolution); therefore, the ADC-212 Picotech Virtual Instrument was used. To ensure that spectral leakage of the FFT results was minimized, the frequency of the source was specified at 9732 Hz to produce a sampled waveform with an integral number of cycles for a sample size of 4096.

Using the optimization software developed by Wilson *et al.* [33], the 3E5 ferrite material was characterized using the original Jiles–Atherton model, with the parameters given in Table II.

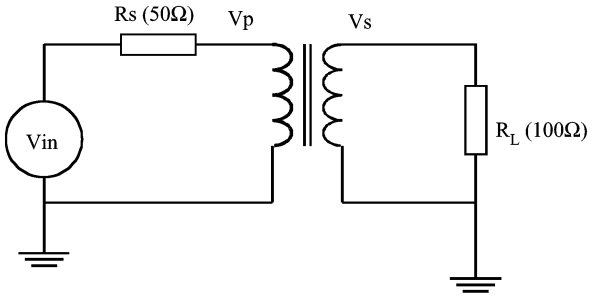

Fig. 16. Transformer THD test circuit.

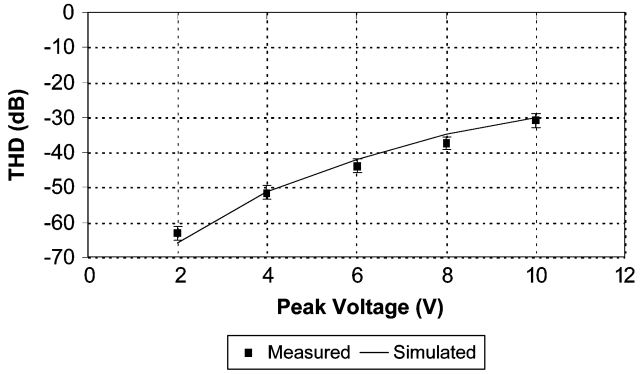

Fig. 17. TN10/6/4-3E5 comparison of measured and simulated THD.

The model was optimized to measured results obtained at approximately the same operating conditions as the THD test circuit to ensure a like-with-like comparison.

The transformer was tested using the circuit shown in Fig. 16, with the peak input voltage varied from 2 to 10 V in 2-V steps. The simulation model was based on the general structure shown in Fig. 8.

The THD calculated for the measured and simulated test circuits is given in Fig. 17.

Using this approach, it is clear that accurate estimates of the THD for transformers can be obtained with the use of suitably characterized material models of the core. In this case, the difference between the measured and simulated results is within 4 dB (worst case) and often within a fraction of a decibel. It was found that if the material was not characterized for the general operating conditions of the transformer, that much less accurate results were obtained, highlighting the necessity for specific material models, or models that change behavior accurately depending on the applied field strength levels.

C. ER11-3E6 Line Transformer

Obviously, the toroid analyzed in the previous section would not be used in practice, but rather a gapped core such as EP13 or ER11. The EP13 cores have been well used in commercial applications but are becoming a significant cost of the hybrid design due to their relatively large size and weight. It was therefore considered useful to investigate the performance of ER11 cores. These cores are significantly smaller, and also offer the potential to be used in planar or thick film constructions as well as the conventional wire wound form. The first test case was a two winding transformer, wire wound on an ER11 two piece ungapped core made of Philips 3E6. Each winding was wound

TABLE III
ER11-3E6 MODEL PARAMETERS

Parameter	Value
a	15.0
k	40.0
c	1.06
α	3.6u
M_s	224k

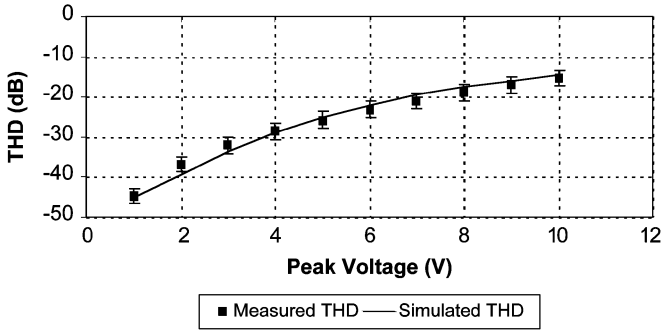

Fig. 18. ER11-3E6 comparison of measured and simulated THD.

with nine turns of 28 s.w.g wire to give an inductance of 230 μH. This transformer was tested using the same test circuit as used previously (shown in Fig. 11). The core was characterized in the same way as the toroid previously described, with the resulting model parameters given in Table III.

The parameters are in a similar range to those for the 3E5 toroid, but it is worth noting that the characterization includes the small gap between the two core halves. The THD of the transformer was measured using the circuit shown in Fig. 16, with the peak input voltage varied from 1 to 10 V in 1-V steps. The THD calculated for the measured and simulated test circuits is given in Fig. 18.

In this case, the core is ungapped, so the THD is relatively poor for this range of input voltage. The addition of a core gap will have the effect of storing energy in the gap rather than the core and hence reducing the effect of the core material nonlinearities on the signal through the transformer. In order to compare the gapped and ungapped behavior, the ER11-3E6 core was tested using the same current applied to the primary winding, with no load attached to the secondary. This method, while not replicating the line conditions, allows a direct comparison of the gapped and ungapped core for a specific current applied to the primary. The primary current was applied across the range 1–7 mA at 10 kHz (approx) as before. The secondary voltage was used to measure the resulting THD of the transformer for the applied current input. This method also allows the calculation and comparison of the B–H curves for each case. In this case, a larger number of turns was chosen (20 : 20) and a small gap was implemented by grinding the center leg flat using emery paper. The change in measured winding inductance was 2.1 mH (ungapped) to 326 μH (gapped).

The resulting measured waveforms were used to characterize the gapped and ungapped core models, with the resulting Jiles–Atherton model parameters given in Table IV (the ungapped core parameters are slightly different to the previously used parameters, due to the different stimulus levels used to characterize the model).

TABLE IV
ER11-3E6 MODEL PARAMETERS

Parameter	Ungapped	Gapped
a	60.0	15.0
k	45.0	20.0
c	0.15	1.06
α	3.6u	3.6u
M_s	224k	224k

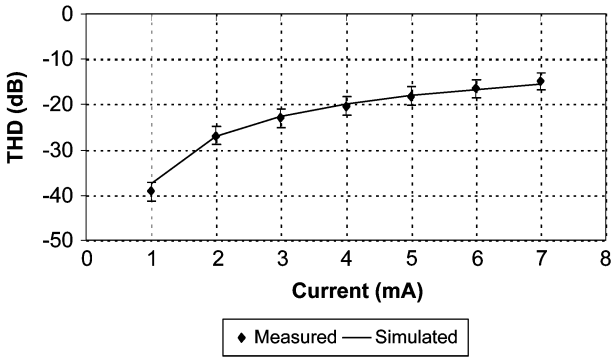

Fig. 19. ER11-3E6 ungapped core (20 turns) measured and simulated THD.

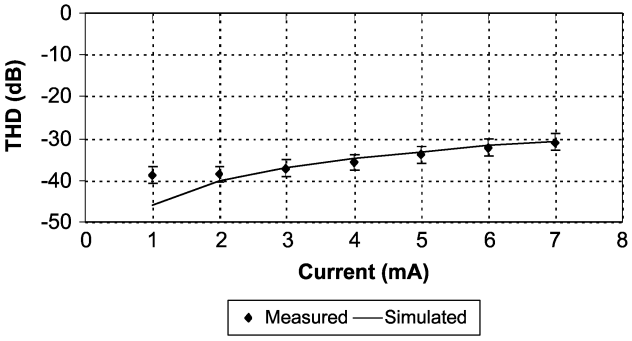

Fig. 20. ER11-3E6 gapped core (20 turns) measured and simulated THD.

The measured values of THD and the values calculated from simulations are summarized in Figs. 19 and 20.

In both cases the correlation is good (within 2 dB), apart from the gapped core at very low current levels. Investigation of this showed that the measured source signal was introducing some noise, limiting the THD achieved. The use of the mixed technology models for measuring the THD from a simulation has been demonstrated to be useful, with the added benefit of insight into the magnetic behavior inside the core. As an illustration of this, Fig. 21 shows the simulated B–H curves inside the gapped and ungapped core models for the same applied current level (7 mA).

As can be seen from the figure, the area of the ungapped core B–H loop is greater and also steeper. This illustrates the effect of the air gap, effectively reducing the effective permeability of the overall core and gap combination. One effect of the introduction of a gap is to effectively reduce the distortion, as more of the energy is stored in the gap.

V. CONCLUSION

This paper has shown how, through the use of mixed-technology magnetic component models, accurate predictions can be made of the THD performance of the device, and that with the added insight that a mixed-domain model brings, design decisions can be made about the geometry and winding configuration using these models with an increased level of understanding about the behavior of the magnetic core.

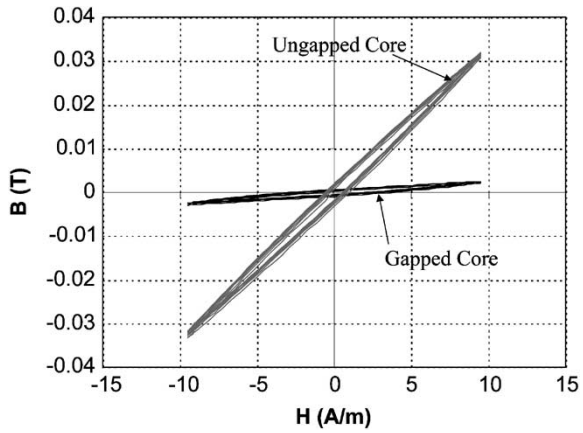

Fig. 21. ER11-3E6 gapped and ungapped core simulated B–H curves.

This work has also demonstrated how effective use can be made of magnetic component models in analyzing the effects of nonlinear magnetics on an electrical circuit or system's behavior.

REFERENCES

[1] *Network and Customer Installation Interfaces—Asymmetric Digital Subscriber Line (ADSL) Metallic Interface*, IEEE Standard T1.413-1995, Aug. 1995.
[2] J. A. C. Bingham, "Multicarrier modulation for data transmission; an idea whose time has come," *IEEE Commun. Mag.*, pp. 5–14, May 1990.
[3] J. M. Cioffi, "A multicarrier primer," ANSI Document, T1413 Technical Subcommittee, (91–157).
[4] W. Goralski, *ADSL and DSL Technologies*, 1st ed. New York: McGraw-Hill, 1998.
[5] W. Y. Chen, *DSL Simulation Techniques and Standards Development for Digital Subscriber Line Systems*. New York: Macmillan, 1998.
[6] B. D. Day, S. Wurcer, and T. Hoffman, "Optimizing line driver designs for maximum power; 'Bridging' ADSL line driver challenges," Analog Devices, Inc., Analog Devices Application Note.
[7] J. P. Cornil, "Building an ADSL modem, the basics," in *Analog Circuit Design—(X)DSL and Other Communications Systems; RF MOST Models; Integrated Filters and Oscillators*. Norwell, MA: Kluwer, 1999, pp. 3–48.
[8] C. D. Cabler, "Survey of the state of the art analog front end circuit techniques for ADSL," in *Analog Circuit Design—(X)DSL and Other Communications Systems; RF MOST Models; Integrated Filters and Oscillators*. Norwell, MA: Kluwer, 1999, pp. 117–126.
[9] M. Steffes, "Optimizing performance in an xDSL line driver," *Electron. Design*, pp. 44–58, Apr. 19, 1999.
[10] E. Nash, "Line-driver design for broadband communications applications," *Electron. Design*, pp. 81–94, Dec. 1, 1997.
[11] D. Dean, "Gain confidence in network designs by simulating the LAN magnetics," Pulse, Inc., Technical Note.
[12] P. L. Dowell, "Effects of eddy currents in transformer windings," in *Proc. Inst. Elect. Eng.*, vol. 113, 1966, p. 1387.
[13] A. Dauhajre and R. D. Middlebrook, "Modeling and estimation of leakage phenomenon in magnetic circuits," in *Proc. PESC'86*, 1986, pp. 213–226.
[14] A. Dauhajre, "Modeling and estimation of leakage phenomena in magnetic circuits," Ph.D. dissertation, California Inst. Technol., Pasadena, CA, 1986.
[15] E. C. Snelling, *Soft Ferrites*, 2nd ed. London, U.K.: Butterworth, pp. 330–335.
[16] R. Asensi, J. A. Cobos, O. Garcia, R. Prieto, and J. Uceda, "New modeling strategy for high frequency transformer windings," in *Proc. IECON*, 1994, pp. 246–251.

[17] ——, "A full procedure to model high frequency transformer windings," in *Proc. IEEE Power Electronics Specialist Conf.*, vol. 2, 1994, pp. 856–863.
[18] ——, "A CAD tool for magnetic components modeling," in *Proc. Amer. Power Electronics Conf. (APEC)*, vol. 1, 1996, pp. 427–433.
[19] P. R. Wilson, "Advanced modeling and simulation techniques for magnetic components," in *Proc. IEE Power Electronics and Variable Speed Drives Conf.*, Sept. 1998, pp. 187–193.
[20] J. M. Lopera, M. Pernia, J. M. Alonso, and F. Nuno, "A complete transformer electric model including frequency and geometric effects," in *PESC'92 Record. 23rd Annu. IEEE Power Electronics Specialists Conf. (Cat. no. 92CH3163-3)*, vol. 2, pp. 1247–52.
[21] R. Prieto, V. Bataller, J. A. Cobos, and J. Uceda, "Influence of the winding strategy in toroidal transformers," in *Proc. IECON*, vol. 1, 1998, pp. 359–64.
[22] R. Prieto, J. A. Cobos, O. Garcia, P. Alou, and J. Uceda, "Taking into account all the parasitic effects in the design of magnetic components," in *Proc. APEC'98*, vol. 1, pp. 400–406.
[23] R. Prieto, J. A. Cobos, O. Garcia, and J. Uceda, "Interleaving techniques in magnetic components," in *Proc. APEC'97*, vol. 2, pp. 931–936.
[24] ——, "Influence of the winding strategy on the parasitics of magnetic components," in *Proc. EPE'97*, vol. 2, pp. 38–43.
[25] J. Tellado, *Multicarrier Modulation with Low PAR*. Norwell, MA: Kluwer, 2000.
[26] "The use of ferrite cores in DSL wideband transformers," Ferroxcube, Inc., Application Note, 2001.
[27] D. C. Jiles and D. L. Atherton, "Theory of ferromagnetic hysteresis (invited)," *J. Appl. Phys.*, vol. 55, pp. 2115–2120, Mar. 1984.
[28] ——, "Theory of ferromagnetic hysteresis," *J. Magn. Magn. Mater.*, vol. 61, pp. 48–60, 1986.
[29] ——, "Ferromagnetic hysteresis," *IEEE Trans. Magn.*, vol. MAG-19, pp. 2183–2185, Sept. 1983.
[30] P. R. Wilson, J. N. Ross, and A. D. Brown, "Optimizing the Jiles-Atherton model of hysteresis using a genetic algorithm," *IEEE Trans. Magn.*, vol. 37, pp. 989–993, Mar. 2001.
[31] P. R. Wilson and J. N. Ross, "Definition and application of magnetic material metrics in modeling and optimization," *IEEE Trans. Magn.*, vol. 37, pp. 3774–3780, Sept. 2001.
[32] P. R. Wilson, J. N. Ross, and A. D. Brown, "Simulation of magnetic component models in electric circuits including dynamic thermal effects," *IEEE Trans. Power Electron.*, to be published.
[33] ——, "Magnetic material model characterization and optimization software," *IEEE Trans. Magn.*, vol. 38, pp. 1049–1052, Mar. 2002.
[34] E. C. Cherry, "The duality between inter-linked electric and magnetic circuits," *Proc. Physics Soc.*, vol. 62, pp. 101–111, 1949.
[35] E. R. Laithwaite, "Magnetic equivalent circuits for electrical machines," *Proc. Inst. Elect. Eng.*, vol. 114, pp. 1805–1809, Nov. 1967.
[36] C. J. Carpenter, "Magnetic equivalent circuits," *Proc. Inst. Elect. Eng.*, vol. 115, pp. 1503–1511, Oct. 1968.
[37] A. D. Brown, J. N. Ross, K. G. Nichols, and M. D. Penny, "Simulation of magneto-electronic systems using Kirchoffian networks," in *Eur. Conf. Magnetic Sensors and Actuators*, Sheffield, U.K., July 1998.
[38] P. R. Wilson, "Modeling magnetic components in electric circuits," Ph.D. dissertation, Univ. Southampton, U.K., 2001.
[39] K. H. Carpenter, "A differential equation approach to minor loops in the Jiles-Atherton hysteresis model," *IEEE Trans. Magn.*, vol. 27, pp. 4404–4406, Nov. 1991.
[40] D. C. Jiles, "A self consistent generalized model for the calculation of minor loop excursions in the theory of hysteresis," *IEEE Trans. Magn.*, vol. 28, pp. 2602–2604, Sept. 1992.

Peter R. Wilson (M'98) received the B.Eng. degree in electrical and electronic engineering and the postgraduate diploma in digital systems engineering from Heriot-Watt University, Edinburgh, U.K., in 1988 and 1992, respectively, the M.B.A degree from the Edinburgh Business School in 1999, and the Ph.D. degree from the University of Southampton, Southampton, U.K., in 2002.

He worked in the Navigation Systems Division of Ferranti plc., Edinburgh, from 1988 to 1990 on fire control computer systems, before moving in 1990 to the Radar Systems Division of GEC-Marconi Avionics, Edinburgh. From 1990 to 1994, he worked on modeling and simulation of power supplies, signal processing systems, servo, and mixed technology systems. From 1994 to 1999, he was a European Product Specialist with Analogy Inc., Swindon, U.K. During this time, he developed a number of models, libraries, and modeling tools for the Saber simulator, especially in the areas of power systems, magnetic components, and telecommunications. He is currently a Lecturer in the Department of Electronics and Computer Science, University of Southampton, and has been working in the Electronic Systems Design Group at the university since 1999. His current research interests include modeling of magnetic components in electric circuits, power electronics, renewable energy systems, VHDL-AMS modeling and simulation, and the development of electronic design tools.

Dr. Wilson is a member of the IEE and a Chartered Engineer in the U.K.

J. Neil Ross received the B.Sc. degree in physics in 1970 and the Ph.D. degree in 1974 for work on the physics of ion laser discharges, both from the University of St. Andrews, U.K.

For 12 years, he worked at the Central Electricity Research Laboratories of the CEGB undertaking research on the physics of high voltage breakdown and optical fiber sensors for use in a high-voltage environment. He joined the University of Southampton, Southampton, U.K., in 1987 and has undertaken research in a variety of fields associated with instrumentation and measurement. He is currently a Senior Lecturer in the Department of Electronics and Computer Science at the University of Southampton. His current research interests include the modeling of magnetic components for communications, instrumentation, and power applications.

Andrew D. Brown (M'90–SM'96) was born in the U.K. in 1955. He received the B.Sc. (Hons) degree in physical electronics and the Ph.D. degree in microelectronics from the University of Southampton, Southampton, U.K., in 1976 and 1981, respectively.

He was appointed Lecturer in Electronics at the University of Southampton in 1981, Senior Lecturer in 1989, Reader in 1992, and was appointed to an established chair in 1998. He was a Visiting Scientist at IBM, Hursley Park, U.K., in 1983 and a Visiting Professor at Siemens NeuPerlach, Munich, Germany, in 1989. He is currently head of the Electronic System Design Group, Electronics Department, University of Southampton. The group has interests in all aspects of simulation, modeling, synthesis, and testing.

Prof. Brown is a Fellow of the IEE, a Chartered Engineer, and a European Engineer.